

Raman and infrared spectra of vitreous As_2O_3

F. L. Galeener, G. Lucovsky, and R. H. Geils

Xerox Palo Alto Research Center, Palo Alto, California 94304

(Received 16 October 1978)

We report the polarized reduced Raman spectra, the infrared reflectivity, and dielectric constants of bulk As_2O_3 glass for vibrational frequencies up to 1500 cm^{-1} . Longitudinal and transverse optical modes are identified in the high-frequency region, as are some features of the second-order response. The atomic motions associated with several lines are inferred from an analogy with the spectra of the tetrahedral glass GeO_2 . Our assignments bring into question the force constants previously deduced by Papatheodorou and Solin. The spectra of bulk As_2S_3 glass and As_2Se_3 glass are also given a parallel interpretation.

INTRODUCTION

The Raman spectra of vitreous (v -) As_2O_3 have been reported previously, most recently by Papatheodorou and Solin (PS),¹ who used the positions of Raman and infrared transmission spectral features to make an analysis based on the combined vibrational modes of AsO_3 pyramidal "molecules" and bent As_2O (waterlike) "molecules." Since that work, Galeener and Lucovsky² have shown that the high-frequency modes of the tetrahedral glasses v - SiO_2 and v - GeO_2 are split into pairs of well-resolved transverse optical (TO) and longitudinal optical (LO) modes. This splitting of high-frequency modes leads to features in the Raman spectra of the tetrahedral glasses which have been the cause for some confusion and error in earlier interpretations of the spectra. Sometimes these extra modes have been ascribed to unidentified impurities, or defects, or have been the reason for postulating unnecessarily complex structures for the glass.

In the present paper we report the polarized Raman spectra, the infrared (ir) reflectivity, and the ir dielectric constants of anhydrous v - As_2O_3 . The ir dielectric constants enable the assignment of several modes as TO or LO in character. We show that while there are significant TO-LO splittings in the vibrational response of v - As_2O_3 , several of these high-frequency modes overlap in the Raman spectra and appear misleadingly as only one broad band that peaks at about 810 cm^{-1} . The spectral features of v - As_2O_3 are then interpreted by analogy with similar ones seen in the vibrational spectra of v - GeO_2 . Finally, we use these results to guide an interpretation of the previously reported spectra of v - As_2S_3 and v - As_2Se_3 . Our clarification of the high-frequency components in v - As_2O_3 implies significant changes in some of the force constants obtained by PS, and has led us to begin an alternative analysis to be reported at a later date.³

EXPERIMENTAL DETAILS

Our samples were made from 99.999% As_2O_3 powder that was first sealed in a silica ampoule, then melted. The ampoule was held in a furnace at 600°C and became fully densified in about 24 h with the aid of slow tilting and turning of the ampoule. Two-mm thick wall coatings of glass were formed by cooling the ampoule in an air blast to about 200°C , at which temperature the material was annealed for several minutes, then cooled slowly to room temperature. Material taken from the ampoule was placed in a disposable plastic glove bag where it was fractured to shape, ground and dry polished ($0.3\text{-}\mu$ alumina), then removed to storage in a desiccated container. The resultant samples showed no optical rotation or inhomogeneity between crossed polarizers. Since the ingestion of quite small amounts of this material is dangerous,⁴ special care was taken not to contaminate the laboratory or sample handling equipment. Although the material is somewhat hygroscopic and its surfaces ultimately devitrify when exposed to the atmosphere, we found that the Raman samples could be exposed to air-conditioned laboratory air (20°C , 50% relative humidity) for many hours before repolishing was required.

The Raman spectra were obtained at room temperature in the 90° configuration with the samples open to the air. No luminescence was observed so the data were obtained conveniently using $\sim 0.75\text{ W}$ of 514.5-nm radiation from a CR-12 Ar^+ -ion laser. The scattered light was collected with $f/1$ optics and the photomultiplier pulses were counted for 10 sec at 5-cm^{-1} intervals. A reference channel stabilized the effective laser intensity to one part in 3000.⁵ The ir reflectance spectra were obtained from samples taken directly from the desiccated container and placed in a Perkin-Elmer Model 180 spectrometer flushed with dry nitrogen. In both the ir and Raman measurements the spectral slit width was less than 5 cm^{-1} .

RAMAN AND INFRARED SPECTRA OF v -As₂O₃

Figure 1 shows our polarized Raman spectra of v -As₂O₃. They are substantially the same as those reported in Ref. 1, except that we have shown more detail in the region above 650 cm⁻¹, including a weak peak at about 1075 cm⁻¹. The principal features will be discussed later, in connection with the *reduced* Raman spectra.⁶

The infrared reflectivity of v -As₂O₃ is shown in Fig. 2; it appears to be the first reported in the literature. Kramers-Kronig analysis of this spectrum⁷ enables computation of the real (ϵ_1) and imaginary (ϵ_2) parts of the complex dielectric constant $\epsilon = \epsilon_1 + i\epsilon_2$. This in turn enables computation of the ir energy-loss function $\text{Im}(-1/\epsilon)$. As we have elaborated elsewhere,² peaks in ϵ_2 indicate the frequencies of TO modes while peaks in $\text{Im}(-1/\epsilon)$ mark those of LO modes.

These ir derived dielectric functions are compared with the *reduced* Raman spectra⁶ in Fig. 3. The solid vertical lines are placed at the frequencies of the two main peaks in ϵ_2 and indicate bands of TO modes centered at 615 and 785 cm⁻¹, the latter being wider than the former. Because it aligns quite well with the major peak in ϵ_2 , we identify the 610-cm⁻¹ Raman band as TO. In contrast, the 795-cm⁻¹ peak in ϵ_2 does not align with the peak of the broad Raman structure at 810 cm⁻¹. The dashed vertical lines, placed at the two most prominent peaks in $\text{Im}(-1/\epsilon)$, indicate a broad band of LO modes at 700 cm⁻¹ and a narrower band at 850 cm⁻¹. Neither of these lines corresponds to a distinct feature in the reduced Raman spectrum. We conclude that the broad Raman structure from ~650 to ~900 cm⁻¹ is the superposition of contributions from three bands, the 700 cm⁻¹ (LO), the 795 cm⁻¹ (TO), and the 850 cm⁻¹ (LO). This structure has the same weak polarization (HH to HV , ~2) as we have observed² for the highest-frequency TO and LO Raman modes in v -GeO₂ and v -SiO₂ [where the Raman

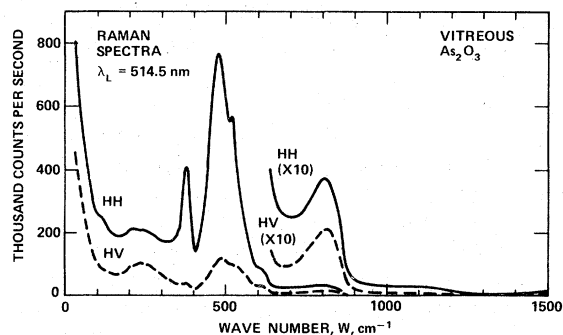


FIG. 1. Polarized Raman spectra of v -As₂O₃.

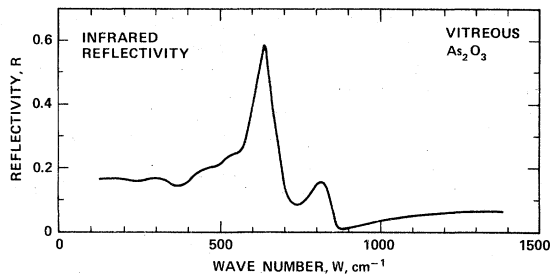


FIG. 2. ir reflectivity of v -As₂O₃.

lines are distinct and correspond to distinct peaks in ϵ_2 and $\text{Im}(-1/\epsilon)$].

The frequencies of the maxima which occur in the first-order HH Raman, HV Raman, ϵ_2 , and $\text{Im}(-1/\epsilon)$ spectra are listed in Table I. Polarization ratios (HH to HV) for the Raman-active modes can be computed directly from the upper panel of

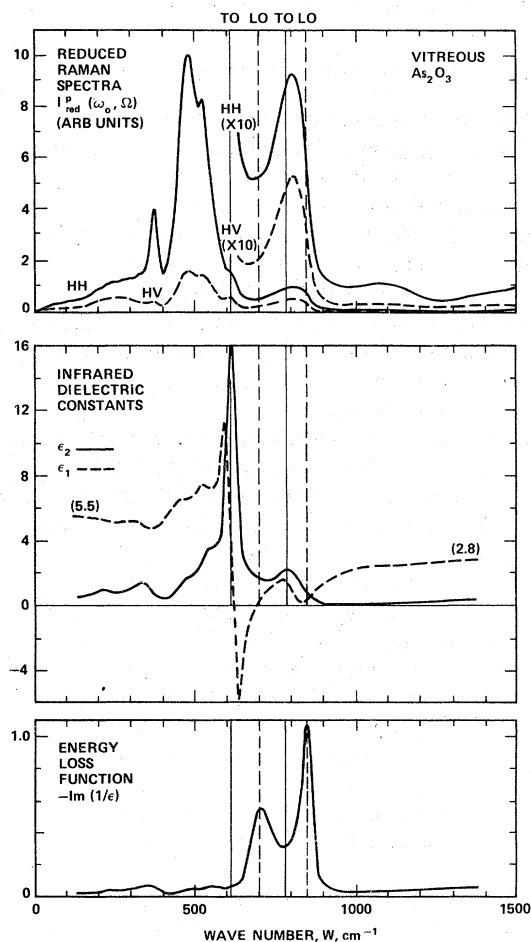


FIG. 3. Reduced Raman spectra, ir dielectric constants, and ir energy-loss function of v -As₂O₃. Vertical lines indicate the position of peaks in ϵ_2 and $\text{Im}(-1/\epsilon)$.

TABLE I. Wave-number (cm^{-1}) positions of identifiable peaks (or prominent shoulders) in the vibrational spectra of $v\text{-As}_2\text{O}_3$ shown in Fig. 3. Positions are arranged in order of ascending frequency, and are segregated into a common vertical column if within $\pm 5 \text{ cm}^{-1}$ of each other. The parentheses indicate peaks that are suspected of arising from two or more overlapping bands.

$I_{\text{red}}^{\text{HH}}$...	(255)	...	378	482	527	...	610	(810)	...	(1090)
$I_{\text{red}}^{\text{HV}}$...	(250)	...	372	485	525	...	612	(810)	...	(1090)
ϵ_2	220	...	335	...	485	...	550	615	...	795
$\text{Im}(-1/\epsilon)$	220	...	342	...	485	...	552	...	700	850	...

Fig. 3.

The broad Raman feature at 1090 cm^{-1} in the reduced spectrum is undoubtedly second-order scattering associated with the strong first-order bands between 400 and 600 cm^{-1} . Although it does not reach maximum at precisely twice the frequency of the main Raman line ($2 \times 485 = 970 \text{ cm}^{-1}$), the relative strength and degree of polarization of this feature are like those that we have reported⁸ for second-order Raman scattering in $v\text{-SiO}_2$.

TO-LO PAIRS AND BARE MODE FREQUENCIES IN $v\text{-As}_2\text{O}_3$

There is no theoretical method for vibrational analysis of glasses which accurately includes the long-range (Coulomb) forces that give rise to the TO-LO splittings.⁹ All available methods produce "bare mode" frequencies, those that would exist if the ir effective charges were zero and only the short-range (bonding) forces were operative. It is therefore important to experimentally determine precisely which LO mode is associated with a given TO mode, and to estimate the bare mode frequency for the pair.

The two pairs in $v\text{-As}_2\text{O}_3$ are 615 cm^{-1} (TO)- 700 cm^{-1} (LO) and 795 cm^{-1} (TO)- 850 cm^{-1} (LO). They are in the normal sequence in which associated modes usually appear, i.e., in ascending vibrational frequency in the order TO-LO, TO-LO, etc., just as we have observed in $v\text{-SiO}_2$ and $v\text{-GeO}_2$.² Occasionally, however, this sequence is modified, as reported, for example, in $v\text{-BeF}_2$.¹⁰ In that case the lower-frequency band of two neighboring TO bands is so strong and wide that its associated LO band lies at frequencies *above* that of the second (weaker) TO band, and the order of the *intervening* pair is reversed, to LO-TO.¹¹ This reversal does not occur in $v\text{-As}_2\text{O}_3$, as is easily seen by inspecting ϵ_2 and ϵ_1 in Fig. 3 while imagining that the 795-cm^{-1} (TO) band does not exist. It is then clear that the ϵ_1 associated with the lower-frequency (615 cm^{-1}) TO mode would still have a zero at about 700 cm^{-1} , and therefore yield a peak in $\text{Im}(-1/\epsilon) = \epsilon_2/(\epsilon_1^2 + \epsilon_2^2)$ at about the same frequency. It follows that the LO mode associated with the 615-cm^{-1} TO mode is at 700 cm^{-1} , not at 850

cm^{-1} .

We have argued elsewhere¹⁰ that the bare mode frequency of a TO-LO pair in the tetrahedral glasses $v\text{-SiO}_2$, $v\text{-GeO}_2$, and $v\text{-BeF}_2$ is nearer the LO than the TO value. Moreover, Galeener¹² has carried out network calculations for these glasses that predict the highest-frequency bare mode to be *very near* the LO value. We therefore tentatively assume that the two highest bare mode frequencies to be used in network, cluster, or molecular calculations for $v\text{-As}_2\text{O}_3$ are better *approximated* by the LO values, 700 and 850 cm^{-1} . The true bare mode frequencies are presumably somewhat less than the LO values.

DISCUSSION OF $v\text{-As}_2\text{O}_3$

The structure of $v\text{-As}_2\text{O}_3$ is presumed to be a continuous random network (CRN) of AsO_3 pyramidal units, each oxygen being shared between two different neighboring pyramids. This is the same topology as is assumed for the structure of $v\text{-As}_2\text{S}_3$ and $v\text{-As}_2\text{Se}_3$. Although more attention has been paid to the chalcogenide glasses, it appears that $v\text{-As}_2\text{O}_3$ is a better substance for testing vibrational models for this kind of CRN: the numerous vibrational modes of the pyramidal CRN overlap in the spectra of the chalcogenide glasses^{13,14} while they are much better separated in the Raman and ir spectra of $v\text{-As}_2\text{O}_3$. This better separation is primarily a result of the greater mass ratio in $v\text{-As}_2\text{O}_3$ [$M(\text{As})/M(\text{O}) = 4.7$] as compared to the corresponding ratio in $v\text{-As}_2\text{S}_3$ (2.3) and $v\text{-As}_2\text{Se}_3$ (0.95).

The highest-frequency feature used by PS in their $\text{AsO}_3\text{-As}_2\text{O}$ molecular analysis was a 627-cm^{-1} line appearing in their Raman spectrum. This corresponds to the lower-frequency (615 cm^{-1}) TO mode of the two that we have identified. (PS assigned the weak Raman peak at $\sim 810 \text{ cm}^{-1}$ to "As₄ linkages"; however, as we will show shortly, modes in this frequency range are integral parts of the network response and should have been accounted for by the $\text{AsO}_3\text{-As}_2\text{O}$ calculations.) According to our analysis the highest frequency used by PS should have been about 850 cm^{-1} (the

LO mode). At the very least this quantitative discrepancy means that the As-O bond stretching force constant (k_1) that they deduced for their model is in serious error. It is quite likely that other force constants and the O-As-O angle are affected, and that the identification of certain observed modes in terms of special motions of AsO_3 and As_2O molecules will be changed.

It would be quite satisfying and informative to see the combined Raman and ir data interpreted according to a proper vibrational calculation carried out for the $v\text{-As}_2\text{O}_3$ network. Here we have in mind any one of the techniques that have been successfully applied to tetrahedral glasses: the large cluster calculations of Bell and co-workers,¹⁵ the Bethe lattice method of Sen and Thorpe¹⁶ (ST), or the cluster Bethe lattice calculations of Laughlin and Joannopoulos.¹⁷ One advantage of these methods over the Lucovsky-Martin molecular model¹⁸ used by PS is that they more realistically account for the coupling of the neighboring AsO_3 units in the CRN. A disadvantage is that these methods involve theoretical and computation-

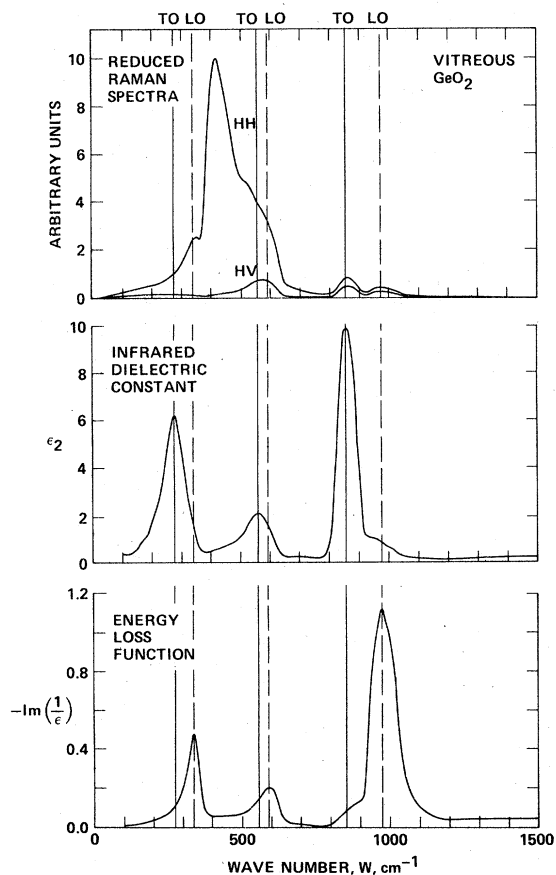


FIG. 4. Vibrational spectra of $v\text{-GeO}_2$, for comparison with those of $v\text{-As}_2\text{O}_3$ in Fig. 3.

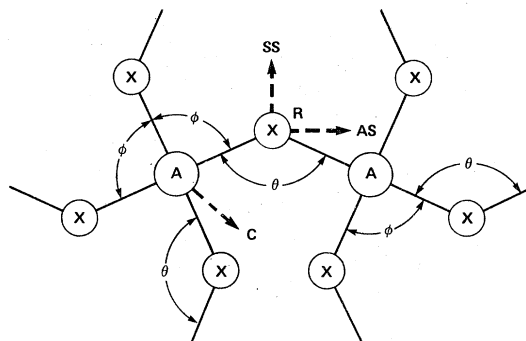


FIG. 5. Schematic diagram of the local order in the ideal CRN for an AX_2 tetrahedral glass such as $v\text{-GeO}_2$.

al facilities often not available.

Since $v\text{-As}_2\text{O}_3$ has not yet been treated by these methods we will pursue several alternative approaches. In the present paper we emphasize analogies that exist between the $v\text{-As}_2\text{O}_3$ spectra and those of the tetrahedral glass $v\text{-GeO}_2$, and use these to infer the atomic motions associated with the main lines in the spectra of $v\text{-As}_2\text{O}_3$. We also make limited use of information to be gained from a recent valence-force-field (VFF) analysis of vibrations in gaseous As_4O_6 ,¹⁹ a molecule which includes *four* coupled AsO_3 "units." In subsequent work³ we will use insight gained from the present analysis to relate the spectra of $v\text{-As}_2\text{O}_3$ to those of the crystalline forms arsenolite and claudite, with emphasis on obtaining more information about the structure of the glass.

Although one does not expect the vibrational spectra of a pyramidal glass to be identical to those of a tetrahedral glass, there are in fact several similarities which we shall delineate and exploit. Since the atomic weight of Ge (72.6) is close to that of As (74.9), it is most useful to compare the vibrational spectra of $v\text{-As}_2\text{O}_3$ with those of $v\text{-GeO}_2$. In Fig. 4 we show the spectra of $v\text{-GeO}_2$ essentially as we have previously reported in Ref.

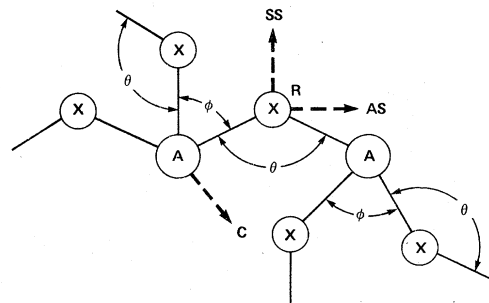


FIG. 6. Schematic diagram of the local order in the ideal CRN for a trigonal pyramidal A_2X_3 glass such as $v\text{-As}_2\text{O}_3$.

2. This is to be compared with the ν - As_2O_3 spectra in Fig. 3.

While the spectra of ν - As_2O_3 and ν - GeO_2 are quantitatively different, they exhibit remarkable *qualitative* similarities. Both materials show three *main* peaks in ϵ_2 , the upper two of which give rise to observable TO-LO splitting [as evidenced in $\text{Im}(-1/\epsilon)$]. Both materials show one *dominant* Raman line, strongly polarized and accounting for more than 50% of the area under the *HH* reduced spectrum, this line is at approximately the same position in both materials, 485 cm^{-1} in ν - As_2O_3 and 420 cm^{-1} in ν - GeO_2 . In each case, two TO-LO pairs lie at frequencies well above this line, and the other TO-LO pair lies below. The higher-frequency TO-LO pairs show up as weak almost unpolarized features (*HH* to *HV*, ~ 2) in the Raman spectra of both materials. Viewed in this way, there is a strong correlation between the number and positions of the main features in the Raman and ir spectra of ν - As_2O_3 and ν - GeO_2 .

Since the atomic motions corresponding to the main features of ν - GeO_2 are now reasonably well understood,^{12, 15-17} the aforementioned spectral similarities make it reasonable to interpret the main features of ν - As_2O_3 in analogy with the interpretation of those of ν - GeO_2 . This will be done with the aid of Figs. 5 and 6, which show schematically the local order for the CRN model of an AX_2 tetrahedral glass (such as ν - GeO_2) and an A_2X_3 trigonal pyramidal glass (such as ν - As_2O_3), respectively. In a first-order discussion, it is assumed that the X - A - X angles ϕ are everywhere the same in a given glass (e.g., 109.5° in the tetrahedral glasses), and that disorder is due primarily to variations in the A - X - A bridging angle θ .

Extending the theoretical work of ST,¹⁶ Galeener¹² has associated the main features of the Raman

and ir spectra of several AX_2 tetrahedral glasses with four principal motions, labeled SS, AS, R , and C in Fig. 5. These "canonical" motions were first defined (using a somewhat different nomenclature) by Bell and co-workers¹⁵ and were also employed by Sen and Thorpe.¹⁶ Here, and in Fig. 6, SS stands for a "symmetric stretch" of the A - X bonds, i.e., motion of the bridging X atom along the line bisecting the A - X - A angle; AS stands for an "antisymmetric stretch" of the bonds, i.e., motion of X along a line parallel to that (A - A) between the two bridged A atoms; R stands for "rocking" motion of X , along a line orthogonal to SS and AS, hence, perpendicular to the A - X - A plane; and C stands for "cation motion" (motion of the A atoms in unspecified directions).¹² In the central force approximations of ST, combinations of these motions account for the principal features of the spectra, as next described.

For ease of reference, we label the four bare mode frequencies of ν - GeO_2 in ascending frequency as ω_0 , ω_1 , ω_3 , and ω_4 . The wave-number positions and primary atomic motions of these bands have been reported elsewhere¹² and are listed in columns (1) and (2) of Table II. The bands corresponding to these peak wave-number values are easily identified in Fig. 4 to be the low-frequency LO-TO pair (ω_0), the dominant Raman band (ω_1), and the two highest-frequency LO-TO pairs (ω_3 , $\omega_4 > \omega_3$). According to our previous correlation of Fig. 4 with Fig. 3, there are similar bands in the spectra of ν - As_2O_3 ; their wave-number values are tabulated in column (3) of Table II.

We thus infer that the ω_0 , ω_1 , ω_3 , and ω_4 bands of ν - As_2O_3 as defined in Table II have atomic motions similar to those listed therein for ν - GeO_2 . There is at least one important difference: we expect more cation (As) motion in the modes of

TABLE II. Center frequencies of *selected* bands ω_i in the vibrational spectra of vitreous GeO_2 , As_2O_3 , As_2S_3 , and As_2Se_3 . In ν - GeO_2 these bands comprise the principal response of the network; the primary motion involved in each band is listed in column (2), using symbols defined in Fig. 5 and the text. The frequencies listed for ν - As_2O_3 , ν - As_2S_3 , and ν - As_2Se_3 are for spectral features showing marked similarity to the ω_i bands in ν - GeO_2 . We infer that the atomic motions corresponding to these bands are similar in all the materials, with qualifications given in the text. The bare mode frequencies for ν - GeO_2 are better approximated by the LO values given, and this may also be true for the other three materials. A few other significant bands are seen in the latter materials, as listed in Tables I, III, and IV.

Band center designation	ν - GeO_2		ν - As_2O_3	ν - As_2S_3	ν - As_2Se_3
	(1) Approximate wave number (cm^{-1})	(2) Primary motion in ν - GeO_2	(3) Approximate wave number (cm^{-1})	(4) Approximate wave number (cm^{-1})	(5) Approximate wave number (cm^{-1})
ω_0 (TO-LO)	278-347	R	335-342	160-170	100-?
ω_1	420	SS	482	340	230
ω_3 (TO-LO)	556-595	SS + C	615-700	308-353	217-235
ω_4 (TO-LO)	857-973	AS + C	795-850	365-390	270-270

v -As₂O₃ because As is *asymmetrically* connected in the v -As₂O₃ CRN, while Si is more symmetrically (tetrahedrally) connected in the v -GeO₂ network. For example, in the central force approximation of ST, ω_1 for v -GeO₂ is pure SS motion, *with no C motion*. In v -As₂O₃ the absence of C motion is unlikely; it appears that phased SS motion must be accompanied by some compensating motion of the As atom.

The analogy with v -GeO₂ does not account convincingly for certain of the weaker features seen in the vibrational spectra of v -As₂O₃. In particular, there are two features at question in the Raman spectra (527 and 378 cm⁻¹) and three at question in the ϵ_2 spectra (550, 485, and 220 cm⁻¹). It is possible that some of these lines reflect essential differences in the vibrational response between four-connected v -GeO₂ and three-connected v -As₂O₃; hence they are worthy of individual discussion.

The weak sharp Raman line seen clearly at 527 cm⁻¹ in v -As₂O₃ may have a counterpart in the "bump" seen at 520 cm⁻¹ on the high-frequency side of the dominant Raman line in v -GeO₂. Galeener²⁰ has shown that the 520-cm⁻¹ bump in v -GeO₂ increases with neutron bombardment of the material and represents a defect structure presumably analogous to that which appears prominently in v -SiO₂ at 606 cm⁻¹.²¹ Neutron bombardment experiments are planned to directly test the hypothesis that the 527-cm⁻¹ line in v -As₂O₃ is also defect related. Nevertheless, the defect hypothesis appears to be weakened in advance by the fact that the 527-cm⁻¹ line suffers little or no change in relative intensity as PS raise their sample temperature from 11.4 to 920 °K.¹ This latter observation suggests that the 527-cm⁻¹ line reflects the basic structure of the glass, or the presence of an unknown impurity.

The 378-cm⁻¹ line in the Raman spectrum of v -As₂O₃ may have a counterpart in the similarly sharp Raman line seen at 347 cm⁻¹ in v -GeO₂, since both align rather well with LO modes revealed in the energy-loss function (342 cm⁻¹ in v -As₂O₃). However, there are problems with this interpretation. In v -As₂O₃ the peak is not as well aligned with the LO mode as is the case in v -GeO₂, and it is appreciably stronger relative to the dominant Raman band. A possible alternative source for this line in v -As₂O₃ is suggested by Raman data on gaseous As₄O₆. Beattie and co-workers²² report two highly polarized lines in the gas, one at 556 cm⁻¹ and the other at 381 cm⁻¹. The atomic motions for these lines are depicted by Sourisseau and Mercier.¹⁹ It is possible that the 378-cm⁻¹ line in the glass represents motions like those involved in the 381-cm⁻¹ mode of the As₄O₆ molecule. We will further explore this possibility

in a later paper.³

The weak peaks in ϵ_2 at 550 and 485 cm⁻¹ align fairly well with peaks in the Raman spectrum; thus they may not represent additional modes, but rather modes which are both Raman and ir active. We have no explanation to offer for the weak peak in ϵ_2 at 220 cm⁻¹.

APPLICATION TO v -As₂S₃

After discovering the TO-LO splittings in v -SiO₂ and v -GeO₂,² we carried out similar ir and Raman experiments on v -GeS₂ and v -As₂S₃.¹³ The spectra for v -As₂S₃ are replotted in Fig. 7, where it is evident that the features between 250 and 450 cm⁻¹ consist of several overlapping bands. The frequencies of the maxima which occur in the *HH* Raman, *HV* Raman, ϵ_2 , and $\text{Im}(-1/\epsilon)$ spectra of v -As₂S₃

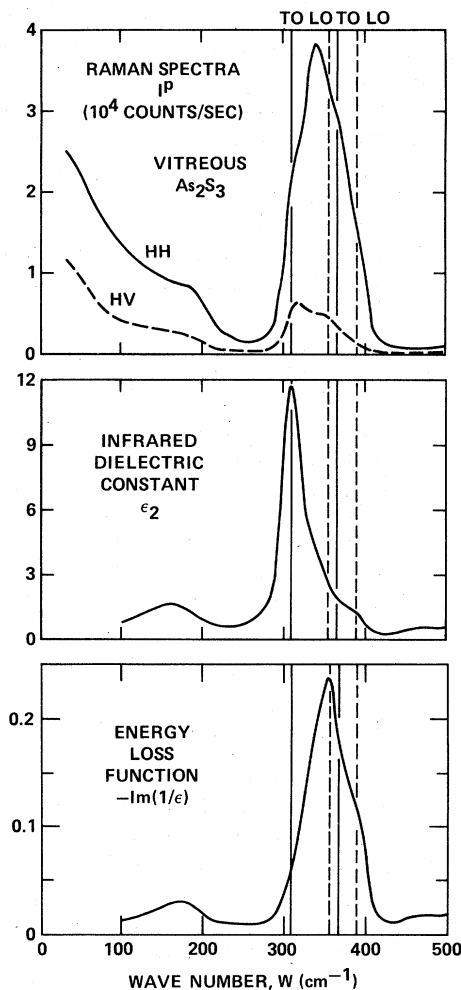


FIG. 7. Polarized Raman spectra, ir dielectric constant ϵ_2 , and ir energy-loss function $\text{Im}(-1/\epsilon)$ of v -As₂S₃. The placement of vertical lines for TO and LO modes is explained in the text.

TABLE III. Wave number (cm^{-1}) positions of identifiable peaks (or shoulders) in the vibrational spectra of $\nu\text{-As}_2\text{S}_3$ shown in Fig. 7. Positions are arranged in order of ascending frequency, and are segregated into a common vertical column if within $\pm 5 \text{ cm}^{-1}$ of each other. The parentheses indicate shoulders whose positions are more uncertain.

I^{HH}	180	(310)	340	...	(365)	...
I^{HV}	315	345	(395)
ϵ_2	160	308	(345)	(390)
$\text{Im}(-1/\epsilon)$...	170	356	...	(390)

are listed in Table III. It was in an effort to clarify the number and nature of the component bands in $\nu\text{-As}_2\text{S}_3$ that we began our study of $\nu\text{-As}_2\text{O}_3$.

Following our analysis of $\nu\text{-As}_2\text{O}_3$, we look for one band in ϵ_2 at low frequencies (possibly split), and thus estimate ω_0 in $\nu\text{-As}_2\text{S}_3$ to be 160–170 cm^{-1} . We also expect to see one dominant Raman line (which is weak in the ϵ_2 spectrum) and readily identify ω_1 as $\sim 340 \text{ cm}^{-1}$. We likewise look for two high-frequency TO-LO pairs. The lower frequency pair is almost certainly 308 (TO)–356 (LO). The higher-frequency LO is presumably the shoulder in $\text{Im}(-1/\epsilon)$ at $\sim 390 \text{ cm}^{-1}$, but there is no definite shoulder in ϵ_2 to indicate the position of the associated TO mode. Since there is a shoulder in the HH Raman spectrum at $\sim 365 \text{ cm}^{-1}$, we tentatively identify the second pair as 365 (TO)–390 (LO). It is on this basis that we have drawn the TO-LO vertical lines in Fig. 7. (We have not mentioned one frequency, the $\sim 180\text{-cm}^{-1}$ Raman line in $\nu\text{-As}_2\text{S}_3$; this peak may be the analog of the 378-cm^{-1} Raman line in $\nu\text{-As}_2\text{O}_3$.)

The principal mode frequencies for $\nu\text{-As}_2\text{S}_3$ are listed in column (4) of Table II. Here, as before, we assume that the bare mode values for ω_3 and ω_4 are better estimated by the LO values. Testing of this assumption and of our detailed assignments in $\nu\text{-As}_2\text{S}_3$ requires a more quantitative treatment than presently available.

APPLICATION TO $\nu\text{-As}_2\text{Se}_3$

In Fig. 8 we show the Raman and ir spectra of $\nu\text{-As}_2\text{Se}_3$. The HH Raman and ϵ_2 spectra were taken directly from the paper by Lucovsky, Nemanich, Solin, and Keezer.¹⁴ The HV spectrum was computed from the HH using the depolarization ratios (HV to HH) given in Ref. 14. The curve of $-\text{Im}(1/\epsilon)$ was obtained by Kramers-Kronig analysis of the reflectivity data given in Ref. 14. The frequencies of peaks and shoulders are tabulated in Table IV. There are fewer distinct features than was the case in $\nu\text{-As}_2\text{O}_3$ and we assume that this is due to increased overlap of the bands.

Following the usual method, we find that the high-frequency TO-LO pairs in $\nu\text{-As}_2\text{Se}_3$ are ap-

proximately 217 (TO)–235 (LO) and 270 (TO)–270 (LO). The absence of an observable TO-LO splitting for the highest-frequency pair is not intrinsically a problem; however, it leaves us without clear explanation for the 280-cm^{-1} shoulder in the HH Raman spectrum. The principal mode frequencies that we thus propose for $\nu\text{-As}_2\text{Se}_3$ are listed in column (5) of Table II.

SUMMARY

We have presented new measurements of the Raman and ir spectra of $\nu\text{-As}_2\text{O}_3$, identified the TO and LO modes, and related the principal bands of

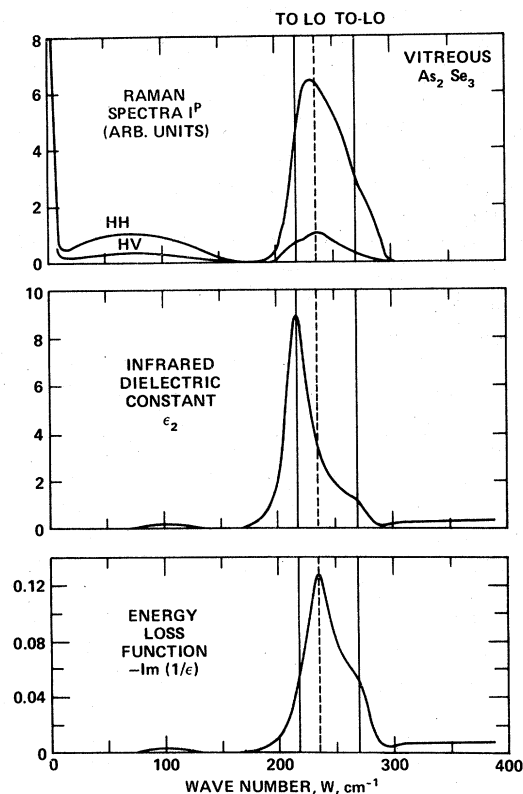


FIG. 8. Polarized Raman spectra, ir dielectric constant ϵ_2 , and ir energy-loss function $\text{Im}(-1/\epsilon)$ of $\nu\text{-As}_2\text{Se}_3$.

TABLE IV. Wave number (cm^{-1}) positions of identifiable peaks (or shoulders) in the vibrational spectra of $\nu\text{-As}_2\text{Se}_3$, deduced from the spectra in Fig. 8. Positions are arranged in order of ascending frequency, and are segregated into a common vertical column if within $\pm 4 \text{ cm}^{-1}$ of each other. The parentheses indicate shoulders whose positions are more uncertain.

J^{HH}	75	230	(280)
J^{HV}	75	...	(215)	...	235
ϵ_2	...	100	217	(270)	...
$\text{Im}(-1/\epsilon)$...	100	235	(270)	...

the spectra to those of the tetrahedral glass $\nu\text{-GeO}_2$. This has resulted in a qualitative interpretation of the atomic motions associated with the principal bands which should prove useful in guiding more quantitative analyses when they become available. A similar analysis has been carried out for $\nu\text{-As}_2\text{S}_3$ and $\nu\text{-As}_2\text{Se}_3$.

ACKNOWLEDGMENTS

The authors are grateful to Mr. W. J. Mosby for his assistance in obtaining and reducing the Raman spectra, and to Dr. R. M. Martin for helpful comments on the manuscript.

- ¹G. N. Papatheodorou and S. A. Solin, *Phys. Rev. B* **13**, 1741 (1976); E. J. Flynn, S. A. Solin, and G. N. Papatheodorou, *Phys. Rev. B* **13**, 1752 (1976).
²F. L. Galeener and G. Lucovsky, *Phys. Rev. Lett.* **37**, 1474 (1976).
³G. Lucovsky and F. L. Galeener (unpublished).
⁴See, e.g., N. I. Sax, *Dangerous Properties of Industrial Materials*, 4th ed. (Van Nostrand, New York, 1975), p. 420.
⁵This system has been described by F. L. Galeener and R. H. Geils, in *The Structure of Non-Crystalline Materials*, edited by P. Gaskell (Taylor and Francis, London, 1977), p. 223.
⁶For definition, see F. L. Galeener and P. N. Sen, *Phys. Rev. B* **17**, 1928 (1978).
⁷T. S. Moss, *Optical Properties of Semiconductors* (Butterworths, London, 1959), p. 25.
⁸F. L. Galeener and G. Lucovsky, in *Light Scattering in Solids*, edited by M. Balkanski, R. C. C. Leite, and S. P. S. Porto (Flammarion, Paris, 1976), p. 641.
⁹R. M. Pick and M. Yvinec, in *Lattice Dynamics*, edited by M. Balkanski (Flammarion, Paris, 1978), p. 459.
¹⁰F. L. Galeener, G. Lucovsky, and R. H. Geils, *Solid State Commun.* **25**, 405 (1978).
¹¹J. F. Scott and S. P. S. Porto, *Phys. Rev.* **161**, 903 (1967).
¹²F. L. Galeener, in *Lattice Dynamics*, edited by M. Balkanski (Flammarion, Paris, 1978), p. 345; *Bull. Am. Phys. Soc.* **23**, 338 (1978); *Phys. Rev. B* **19**, 4292 (1979).

- (1979).
¹³For ir spectra of $\nu\text{-As}_2\text{S}_3$, see G. Lucovsky and F. L. Galeener, in *Structure and Properties of Non-Crystalline Semiconductors*, edited by B. T. Kolomiets (Nauka, Leningrad, 1976), p. 207; for Raman spectra, see F. L. Galeener and G. Lucovsky, *ibid.* p. 305.
¹⁴For ir and Raman spectra of $\nu\text{-As}_2\text{Se}_3$, see G. Lucovsky, R. J. Nemanich, S. A. Solin, and R. A. Keezer, *Solid State Commun.* **17**, 1567 (1975).
¹⁵Reviewed by R. J. Bell, in *Methods in Computational Physics*, edited by G. Gilat (Academic, New York, 1976), p. 215.
¹⁶P. N. Sen and M. F. Thorpe, *Phys. Rev. B* **15**, 4030 (1977).
¹⁷R. B. Laughlin and J. D. Joannopoulos, *Phys. Rev. B* **16**, 2942 (1977).
¹⁸G. Lucovsky and R. M. Martin, *J. Non-Cryst. Solids* **8-10**, 185 (1972).
¹⁹C. Sourisseau and R. Mercier, *Spectrochim. Acta A* **34**, 173 (1978); A. Müller, B. N. Cyvin, S. J. Cyvin, S. Pohl, and B. Krebs, *Spectrochim. Acta A* **32**, 67 (1976).
²⁰F. L. Galeener (unpublished). Also quoted in Ref. 21.
²¹For a recent discussion, see F. L. Galeener, J. C. Mikkelsen, Jr., and N. M. Johnson, in *The Physics of SiO₂ and Its Interfaces*, edited by S. T. Pantelides (Pergamon, New York, 1978), p. 284.
²²I. R. Beattie, K. M. S. Livingston, G. A. Ozin, and D. J. Reynolds, *J. Chem. Soc. A*, 449 (1970).